A critical approach to the toxic metal ion removal by hazelnut and almond shells

Salvatore Cataldo[a], Antonio Gianguzza[a], Demetrio Milea[b], Nicola Muratore[a], Alberto Pettignano[a*] and Silvio Sammartano[b]

[a]Dipartimento di Fisica e Chimica, Università di Palermo, Viale delle Scienze, I-90128 Palermo, Italy

[b]Dipartimento di Scienze Chimiche, Biologiche, Farmaceutiche ed Ambientali, Università degli Studi di Messina, Viale Ferdinando Stagno d'Alcontres, 31, I-98166 Messina (Vill. S. Agata), Italy.

* Corresponding author: Tel: +39-091-23897959; Fax: +39-091-590015;

E-mail address: alberto.pettignano@unipa.it

ABSTRACT

The adsorption capacity of ground hazelnut (HS) and almond (AS) shells towards Pb(II) and Cd(II) has been studied at pH=5, in $NaNO_3$ and NaCl ionic media, in the ionic strength range 0.05-0.5 mol L^{-1}. Kinetic and equilibrium experiments were carried out by using the Differential Pulse Anodic Stripping Voltammetry technique to check the amount of the metal ion removed by HS and AS materials. Different kinetic and equilibrium equations were used to fit experimental data and a statistical study was done to establish the suitable model for the data fitting.

A speciation study of the metal ions in solution was also done in order to evaluate the influence of the ionic medium on the adsorption process. TGA-DSC, FT-IR and SEM-EDX techniques were used to characterize the adsorbent materials. The mechanism of metal ions adsorption was explained on the basis of the results obtained by the metal ions speciation study and the characterization of materials.

Keywords: Adsorption, lead(II), cadmium(II), almond shells, hazelnut shells; voltammetry.

1. Introduction

The possibility of using low-cost materials in the metal sorption processes is acclaimed since many years (Volesky 2003; Fu and Wang 2011). Among these materials, residuals and wastes of agriculture products, being totally inexpensive and of biological nature, are considered for their efficiency in the toxic metal removal from aqueous solutions. Several data on the metal sorption by agricultural wastes are reported in the literature (Demirbas 2008; Nurchi and Villaescusa 2008; Nguyen et al. 2013; Kim et al. 2015) and, in particular, rice, olive stones and leaves, bark and cork from different plant species (Volesky 2003; Zhang et al. 2014; Şen et al. 2014; Blázquez et al. 2015; Kim et al. 2015; Monji et al.

2016). Recently, the possibility of using hazelnut, almond, walnut and peanut shells as low cost and eco-friendly sorbent materials has attracted the attention of many research groups (Cimino et al. 2000; Bulut and Tez 2007; Mehrasbi et al. 2009; Pehlivan et al. 2009; Ronda et al. 2013; Taşar et al. 2014; Şencan et al. 2015). Furthermore, another criterion to be considered in the choice of these materials is the local availability. Italy is one of the main almond world producers and the second hazelnut producer (11% of world production in 2014) (Micke 1996; INC International 2015). Their production is mainly located in South Italy and, mainly, in Sicily where a large amount of fruit shells resulting from the fruit treatment of food industry is available and cheap.

As an extension of our previous investigations on the metal ions sorption by different biomaterials (Cataldo et al. 2013b, a, 2015, 2016b), here we report a study on the Pb(II) and Cd(II) ions removal from aqueous solutions by sorption onto ground shells of almonds and hazelnuts harvested in Nebrodi and Madonie mountains in Sicily.

Among toxic metal ions, Pb(II) and Cd(II) are extensively studied, due to their well-known negative effect towards plants, animals and humans (Crompton 2006; Crea et al. 2013). In the last decades our research group carried out a systematic study on the chemical speciation of the two metal ions in different experimental conditions (De Stefano et al. 2010; Cataldo et al. 2012). The formation of the different metal species depends on the conditions and the composition of the solution, *i.e.* medium composition (possible presence of inorganic and organic ligands), ionic strength, temperature, pH. These parameters must be carefully considered in order to adopt the most appropriate conditions to obtain a satisfactory removal of metal ions from aqueous solutions by sorption process. Unfortunately, the speciation studies are often neglected in the literature papers dealing with metal removal using sorbent materials, including AS and HS (Cimino et al. 2000; Bulut and Tez 2007; Mehrasbi et al. 2009; Pehlivan et al. 2009; Şencan et al. 2015).

With the aim to simulate the conditions of most natural and waste waters, in this paper the adsorption capacity of Sicilian ground hazelnut and almond shells towards lead and cadmium ions has been evaluated in aqueous NaCl medium at pH = 5 and in a wide ionic strength range ($0.05 \leq I$ / mol $L^{-1} \leq 0.5$). Measurements in $NaNO_3$ medium were also carried out for comparison.

The AS and HS materials have been characterized by TGA-DSC, SEM-EDX and FT-IR measurements. Kinetic and equilibrium adsorption experiments were carried out evaluating the amount of metal ion adsorbed by Differential Pulse Anodic Stripping Voltammetry (DP-ASV) technique. The experimental data were processed with the models usually employed in literature to fit the kinetic (pseudo-first order, pseudo-second order and Vermeulen) and the isotherm (Freundlich, Langmuir and Sips) data (Park et al. 2010). The Akaike Information Criterion-AIC, and F-test have then been used to compare various fitting functions in order to check for statistically significant

differences between various models (Akaike 1974; OriginLab 2004; Wagenmakers and Farrell 2004; Cataldo et al. 2016a) and refs therein.

2. Materials, methods and procedures

2.1. Reagents

Cd(II) and Pb(II) ion solutions were prepared by weighing the $Cd(NO_3)_2\ 4H_2O$ and the $Pb(NO_3)_2$ (Aldrich, analytical grade) salts, respectively. NaCl and $NaNO_3$ salts (Riedel-de Haën, puriss.) used to set the ionic strength of the solutions were weighed after drying in oven at 110°C for 2 hours. Hydrochloric and nitric acids and sodium hydroxide solutions used to adjust the pH of the metal ion solutions and to calibrate the ISE-H^+ electrode were prepared by diluting concentrated Fluka ampoules. Standard solutions of Pb(II) and Cd(II) ions used for calibration curves were prepared by diluting 1000 mg L^{-1} standard solutions in 2 % HNO_3 (C±0.2% - trace select qualities, Fluka). All the solutions were prepared using freshly, CO_2-free ultra-pure water (ρ ≥18 MΩ cm^{-1}) and grade A glassware.

2.2. Preparation and characterization of adsorbent materials

Almonds (AS) and hazelnuts (HS) shells were obtained from the common almond, *Prunus dulcis* and common hazelnut, *Corylus avellana*, cultivated in the provinces of Palermo and Messina (Sicily). 2 kg of each fruit were shelled and the shells were washed three times with distilled water and then ground by a laboratory mill. The ground shells were sieved for 30 minutes with a sieve shaker Octagon Digital (Endecotts) in order to collect the fractions with the following particle size intervals:

- $0.40 \leq x$ / mm < 1.18 (denoted as “small size” along the manuscript)
- $1.18 \leq x$ / mm < 1.40 (denoted as “big size” along the manuscript)

The ground shells were previously washed several times with distilled water and dried in oven at 50°C.

Known amounts of dried AS and HS were incinerates in muffle at 900 °C to quantify the inorganic fraction. The ash weight was measured after a constant weight was reached. The procedure was repeated on five samples and the mean values ± std. dev. have been reported.

A portion of the shells was ground and sieved in order to obtain a material with a smaller particle size (<200 μm) to be used in TGA-DSC, FTIR and SEM-EDX analysis.

TGA-DSC experiments were performed by using a STA 449 Jupiter F1 (NETZSCH) equipped with Silicon Carbide furnace, DSC sample carrier type S and alumina crucible by 85μL in static air with protective nitrogen flow of 60 mL min^{-1}, in the range 30 - 900°C at heating rate of 10 °C/min. The

sample weight was ca. 10 mg. In DSC measurements heat flow was calculated assuming sensitivity (μV/mW) to be 1.

The investigation on the morphology of the shell powders, before and after contact with the Pb(II) or Cd(II) solutions, was carried out by an electronic microscope ESEM FEI QUANTA 200F coupled with an EDX (Energy Dispersive X-ray spectroscopy) system. Before the analysis the shell powders were oven-dried at T = 105°C for 24 hours. The electron beam was properly set to avoid the damage of the samples. FT-IR measurements (Perkin Elmer Frontier FT-IR spectrometer) were performed on KBr pellets of the almond and hazelnut shell powder before and after 12 hours contact with solutions containing 100 mg of shell powder and the metal ions ($C_{Pb^{2+}}$ or $Cc_{d^{2+}}$ = 30 mg L^{-1} , at pH = 5) under investigation. Samples for FT-IR investigations were dried for three days at 40°C before the use. Pellets were prepared by mixing 2 mg of the sample powder with 140 mg of KBr dried in oven at 105°C. Then the mixtures were mixed in an agate mortar to obtain a homogeneous fine powder and pressed at 12 tons for ca. 10 min. Spectra were recorded at a resolution of 4 cm^{-1} and they are reported as percent of transmittance (T%) *vs* wave number (λ^{-1}) after baseline correction process.

2.3. Procedures for kinetic and equilibrium experiments

The kinetic experiments for Pb(II) or Cd(II) ions adsorption by the small and big sizes HS and AS were carried out in NaCl aqueous solution, at I = 0.1 mol L^{-1} and T = 25°C. The initial pH of the solution was adjusted at 5 and was monitored during the experiments. 0.1 g of HS or AS were added to 25 mL of solution containing the metal ion ($C_{Pb^{2+}}$ or C_{Cd}^{2+} = 30 mg L^{-1}) in a voltammetric cell under constant and regular stirring. The metal ion concentration in solution was measured at various adsorbent/solution contact times in the interval 0 - 360 minutes.

The adsorption isotherm experiments were carried out at the same pH and temperature of the kinetic ones, in NaCl medium, in the ionic strength range $0.05 \leq I$ / mol $L^{-1} \leq 0.50$ and in $NaNO_3$ medium at I = 0.1 mol L^{-1}. Moreover, further adsorption isotherm experiments were carried out for each metal – adsorbent system at T = 40 and 60 °C, at the same pH, in $NaNO_3$, at I = 0.1 mol L^{-1}.

For each isotherm experiment, different amounts of small size HS or AS (0.1 – 1.5 g) were placed in ten Erlenmeyer flasks containing each 20 mL of Pb(II) or Cd(II) solution ($C_{Pb^{2+}}$ or C_{Cd}^{2+} = 30 - 60 mg L^{-1}). The solutions were stirred at 180 rpm for twelve hours using an orbital mixer (model M201-OR, MPM Instruments) in a thermostatted chamber (at T = 25, 40 and 60 °C), and then were separated from the adsorbent before measuring the metal ion concentration and the pH. The residual Pb^{2+} or Cd^{2+} ion concentration in solutions, collected during the experiments, was determined by DP-ASV technique. The voltammetric apparatus consisted of a Metrohm 663 VA stand, combined with the Autolab potentiostat coupled with the IME663 interface. The voltammetric apparatus was controlled

by NOVA v. 1.10 software. The VA stand was equipped with a three electrode system consisting of i) a Multi Mode Electrode Pro (Metrohm, code 6.1246.120) working in the Static Mercury Drop Electrode (SMDE) mode, ii) a glassy carbon auxiliary electrode (code 6.1247.000), and iii) a double junction Ag/AgCl/KCl (3 mol L^{-1}) reference electrode (code 6.0728.030). The DP-ASV measurements were performed after bubbling purified N_2 gas into the solutions for 150 s. The experimental electrochemical conditions (see Table 1S of Supplementary Material) were chosen in order to optimize the quality parameters, such as signal/noise ratio, repeatability, accuracy, and to avoid interferences.

Calibration curves of Pb^{2+} and Cd^{2+} ions were obtained in the same experimental conditions of kinetic and thermodynamic adsorption experiments. The pH of the Pb^{2+} and Cd^{2+} solutions was measured by a potentiometer equipped with a combined ISE-H^+ glass electrode (Ross type 8102). The ISE-H^+ electrode was previously calibrated, in the same experimental conditions of the adsorption experiments, titrating 25 mL of HCl standardized solutions with NaOH. A potentiometric titration system (Metrohm, Model 888 Titrando) controlled by TIAMO software was used.

2.4. Models for kinetic and equilibrium studies of $Pb^{2+}$and Cd^{2+} adsorption

The adsorption kinetics of Pb(II) and Cd(II) were studied using the pseudo-first order (PFO, eq. 1), the pseudo-second order (PSO, eq. 2) and the Vermeulen (Ver, eq. 3) kinetic equations (Ho and Ofomaja 2006; Park et al. 2010):

$$\frac{dq}{dt} = k_1(q_e - q_t) \quad (1)$$

$$\frac{dq}{dt} = k_2(q_e - q_t)^2 \quad (2)$$

$$\frac{dq}{dt} = k_v\frac{(q_e^2 - q_t^2)}{q_t} \quad (3)$$

Their integrated forms, for the boundary conditions $t = 0$, $q = 0$ and $t = t$, $q = q_t$ are reported in eqs 4 – 6:

$$q_t = q_e(1 - e^{-k_1 t}) \quad (4)$$

$$q_t = \frac{q_e^2 k_2 t}{1 + q_e k_2 t} \quad (5)$$

$$q_t = q_e(1 - e^{-2k_v t})^{0.5} \quad (6)$$

where k_1, k_2 and k_v are the rate constants of adsorption, q_e is the sorption capacity at equilibrium and q_t is the amount of metal adsorbed at time t.

Different models were used to correlate and to compare the experimental adsorption equilibrium data

in order to provide an accurate fit for all the adsorption isotherms. In particular, the Freundlich, Langmuir and Sips isotherm models (Ruthven 1984; Park et al. 2010) have been used in the forms reported in eqs 7-9:

$$q_e = K_F C_e^{1/n} \quad (7)$$

$$q_e = \frac{q_m K_L C_e}{1 + K_L C_e} \quad (8)$$

$$q_e = \frac{q_m K_S C_e^{1/S}}{1 + K_S C_e^{1/S}} \quad (9)$$

where q_m is the maximum adsorption capacity of the material expressed in mg g^{-1}; K_F, K_L and K_S are the constants of Freundlich, Langumir and Sips models, respectively; C_e (mg L^{-1}) is the metal concentration in solution at equilibrium, and n and s are empirical parameters. K_F, K_L and K_S are an expression of the the binding capacity or affinity of the adsorbent toward the metal ion, whereas n and s give information on the strength of the adsorption. Langmuir model describes the adsorption on equivalent sites of the adsorbent material that can be saturated obtaining a monolayer, Freundlich model takes in to account the heterogeneity of the binding sites, while both the heterogeneous adsorption and the saturation condition are taken in to account in the Sips model.

The metal ion adsorption capacity at different contact times t (q_t, mg g^{-1}) in the kinetic study, or at different metal / adsorbent ratio in the equilibrium study (q_e, mg g^{-1}) was calculated by the eq. 10:

$$q_t or\ q_e = \frac{V(C_0 - C_t)}{m} \quad (10)$$

where V (L) is the volume of the metal solution and m is the mass of almond or hazelnut shells (grams); C_0 and C_t are the metal ion concentrations in solution (mg L^{-1} of Pb^{2+} or Cd^{2+}) at $t = 0$ and $t = t$, respectively. At the equilibrium condition, eq. 10 was applied by replacing C_t with C_e to calculate q_e.

2.5. Statistical comparison and selection of the best kinetic and thermodynamic models

Different equations and models used to fit the kinetic and the equilibrium data have been statistically compared by common tests, namely the classical Fisher-Snedecor F-test and the Akaike Information Criterion (AIC) (Akaike 1974; OriginLab 2004; Wagenmakers and Farrell 2004; Militky and Meloun 2011; Cataldo et al. 2016a) and refs therein.

The simplest form of the F-test (others may be used) compares the variances (σ_A^2 and σ_B^2) obtained by the fitting of a given dataset by two models:

$$F_{obs} = \frac{\sigma_A^2}{\sigma_B^2} \quad (11)$$

where $\sigma_A^2 > \sigma_B^2$ (the choice of model A or B as numerator is not really influent, since the function 1 / F follows the same distribution of F). If the two models are statistically equivalent (H_0, the null

hypothesis) at a given significance level (α), *i.e.*, $\sigma_A^2 = \sigma_B^2$, it is $F_{obs} < F_{crit}$, where F_{crit} is the critical value for the acceptance of H_0 at a given α and for given d.f.$_A$ and d.f.$_B$ (d.f. are the degrees of freedom, given by the difference between number of points of the dataset, N, and the number of parameters, p, refined by the model). Despite its simplicity, the F-test has some well known limitations including the fact that, rigorously, it would only be suitable to compare nested models (Cataldo et al. 2016a) and refs therein. Moreover, F-test doesn't give any "measure" of the adequacy of a model with respect to another and, in all the cases where differences between two models are not statistically significant at a given level (as it may happen, including some cases in this work), it doesn't help in the model selection. For these purposes, the Akaike Information Criterion (AIC) is "a popular method for comparing the adequacy of multiple, possibly non-nested models". According to AIC, it is possible to calculate an AIC value for each equation used to fit a given dataset (Wagenmakers and Farrell 2004; Cataldo et al. 2016a) and refs therein:

$$AIC = N \ln\left(\frac{RSS}{N}\right) + 2K \quad \text{for} \quad \frac{N}{K} \geq 40 \tag{12a}$$

$$AIC = N \ln\left(\frac{RSS}{N}\right) + 2K + \frac{2K(K+1)}{N-K-1} \quad \text{for} \quad \frac{N}{K} < 40 \tag{12b}$$

with $K = p + 1$ and where RSS is Residual Sum of Squares. For a given dataset, the model with the lowest AIC value is the "best" one. Besides, a more "elegant" approach than the simple comparison of AIC values is via the calculation of the Akaike's weights (*Akw*), "which can be interpreted as conditional probabilities for each model" (higher *Akw* values mean better models):

$$Akw = \frac{e^{(-0.5\,\Delta AIC)}}{(1 + e^{(-0.5\,\Delta AIC)})} \tag{13}$$

where ΔAIC is the difference between AIC values of two models. Interestingly, Akaike's weights can also be calculated to compare a series of M models simultaneously

$$Akw_i = \frac{e^{(-0.5\,\Delta AIC_i)}}{\sum_{i=1}^{M} e^{(-0.5\,\Delta AIC_i)}} \tag{14}$$

where $\Delta AIC_i = AIC_{min} - AIC_i$ (AIC_{min} is the lowest AIC value among those of all M models) and with $\sum Akw_i = 1$. Independently of that, the probability that the model with the lowest AIC value is better than another (with AIC_i) can be calculated both by the AIC or by the *Akw*, as follows:

$$e^{(-0.5\,\Delta AIC_i)} \tag{14a}$$

$$\frac{Akw_i}{Akw_{min}} \tag{14b}$$

3. Results and discussion

3.1. Analysis of adsorbent materials

The ash content of AS and HS materials resulted to be 0.44 ± 0.02 and 0.66 ± 0.03 %, respectively.

The TGA-DSC curves of both AS and HS (Fig. 1) show the characteristic thermal degradation profile of a biomass in presence of air, with three steps relative to: i) the loss of humidity (low temperature region T < 200 °C), ii) the complete decomposition of hemicellulose and cellulose and partial decomposition of lignin (200 ≤ T (°C) ≤ 370), and iii) the decomposition of the remaining lignin and the char oxidation (T (°C) ≥ 370) (Skreiberg et al. 2011). A comparable mass loss and endothermic peaks are shown in the first step of the thermograms, while some differences are found in the second and third steps of TGA and DSC curves. In particular, the third step ends at 580 and 900 °C for HS and AS, respectively. The TGA curves are comparable with those reported in literature for the two materials (Allouch et al. 2014; Kocabaş-Atakli et al. 2015) and the differences in thermal degradation between AS and HS can be ascribed to the different composition in cellulose, hemicellulose, and lignin of the two lignocellulosic materials, with a higher lignin content in the latter, in perfect agreement with literature findings (Cimino et al. 2000; Demirbaş 2002; Pehlivan et al. 2009). In fact, though the lignocellulosic composition of HS and AS shells strictly depends on the cultivar and the place of cultivation, HS usually contains higher amounts of lignin, whereas the structure of AS is mainly constituted by cellulose. DSC curves support the TGA insights. Indeed, the presence of a broad peak in the temperature range 200-580 °C for DSC curve of HS can be mainly attributed to the combustion of a significant quantity of lignin for which exothermic process is expected also in a limited amount of oxygen (Ramiah 1970). A similar DSC curve for HS of Turkish origin was found by other authors (Haykiri-Acma and Yaman 2012). As regards the DSC curve of AS, the endothermic peak at about 375 °C can be primarily attributed to the degradation of cellulose in a poorly oxidizing environment (Martin et al. 2010).

In order to verify metal ion absorption and to check for possible changes in the structure of the materials surface, SEM micrographs of both AS and HS at 250x magnification have been performed before and after contact with Pb(II) or Cd(II) solutions, and are reported in Figs 2(a-b) and in Figs 1S and 2S of Supplementary Material together with the corresponding EDX spectra. As observed, the adsorption of the metal ions does not cause relevant changes in the surface texture of the materials, while semi-quantitative results from EDX spectra (please remember that EDX does not quantify lighter elements, such as H and N) clearly demonstrate metal ions sorption onto the materials surface. The relative composition of HS and AS, calculated in % (w/w) by the EDX before and after contact with Cd(II) or Pb(II) solutions (30 mg L^{-1}, in NaCl 0.1 mol L^{-1} and at pH = 5) is reported in Table 1. From their analysis, it is possible to affirm that:

- HS shows higher affinity towards Pb(II) than Cd(II);

- there is little or no difference in the adsorption of the two metal ions onto AS material;
- AS is a better sorption material for Cd(II) than HS;
- both AS and HS materials show similar sorption characteristics for Pb(II) ion.

HS and AS were also characterized by FT-IR analysis in order to determine which functional groups were responsible for metal sorption. The IR spectra of HS and AS are shown in Fig 3, and are very similar, since, as reported in literature, the three lignocellulosic shell components are all rich of O-donor functional groups (mainly hydroxyl groups), which are responsible for their ability to bind metal ions from aqueous solutions (Cimino et al. 2000; Demirbaş 2002; Pehlivan et al. 2009).

The little differences of peak intensities of some bands are attributable to a different ratios between cellulose, hemicellulose and lignin in the two materials and, in particular, they confirm the higher presence of lignin in HS (Cimino et al. 2000; Demirbaş 2002; Pehlivan et al. 2009). The peaks at ca. 3410 and 2900 cm^{-1} reveal the presence of hydroxyl and C–H groups, respectively, which are abundant in the cellulosic portion and lignin. Bands at 1635 and 1740 cm^{-1} can be ascribed at free and esterified carboxyl groups, respectively, while the strong absorbance centered at 1045 cm^{-1}can be assigned to the C–O. These results confirm those of other authors (Pehlivan et al. 2009; Ronda et al. 2013; Şencan et al. 2015) and let us suppose that both interaction of metal ions on electron donor sites and ionic exchange processes can be simultaneously involved in the adsorption phenomena.

3.2. Characterization of metal species in NaCl aqueous solution – Metal speciation

In addition to the characteristics of sorbent materials, the chemical behavior of metal ions in solution must be investigated to select the most appropriate conditions to reach the best performances in the sorption process. Since the metal sorption mechanism generally occurs by complexation, chelation or ion exchange, the knowledge of the metal species formed (and their charge) as function of both pH and ionic medium composition is fundamental, because each species would interact differently with the binding sites of sorbent materials. In our case, differently charged hydroxo- and chloride- species [$Me(OH)_n^z$ and $MeCl_n^z$, n = 0 to 4, z = from 2+ to 2-] can be formed for both Pb(II) and Cd(II) ions in NaCl aqueous solution. The formation and distribution of metal species (*chemical speciation*) have been investigated using the stability constants reported in the literature (Baes and Mesmer 1976; Crea et al. 2013) and the corresponding distribution diagrams were drawn by ES4ECI computer program (De Stefano et al. 1997). As an example, the distribution diagrams of species formed by Cd(II) and Pb(II) ions in NaCl aqueous solution, at I = 0.1 mol L^{-1} and T = 25°C, are reported in Fig. 4. The species reported in the two diagrams refer to the equilibrium (M^{2+} = Pb^{2+} or Cd^{2+}):

$$M^{2+} + p\ Cl^- + q\ H_2O = MCl_p(OH)_q + q\ H^+$$

Speciation diagrams were also drawn at each investigated ionic strength, as well as without ionic medium (at $I \rightarrow 0$ mol L^{-1}). The corresponding formation percentages of the Cd(II) and Pb(II) species are reported in Table 2S.

The results obtained from metal speciation studies allow us to make the following considerations:

- as expected, the formation of chloride species for both Pb(II) and Cd(II) ions becomes relevant when NaCl concentration increases, with a consequent lowering of free metal ions in solution;
- chloride complexation determines a change in the charge of the metal ion species, from positive (2+) to negative (-) in the Pb(II) system and from positive (2+) to neutral 0 in the Cd(II) system;
- No formation of hydroxo species is noted at pH = 5 for both metal ions, confirming the correct choice of this pH value for sorption process.

These results cannot be neglected and must be taken into account during data analysis of the metal adsorption onto HS and AS materials.

3.3. Data analysis of the adsorption kinetics

The kinetics of Pb(II) and Cd(II) adsorption onto small and big particle sizes AS and HS materials was studied in $NaCl_{aq}$ at I = 0.1 mol L^{-1}. The materials are in the typical size range of the most used ion exchange resins and adsorbent materials (0.7-1.5 mm) (Volesky 2003). PFO, PSO and Ver kinetic models were used to fit the experimental data, and the sorption parameters of the equations are reported in Table 2 together with their errors, the correlation coefficients, the standard deviation and the Akaike's values of the fits. Fig. 5 and Figs 3S – 5S report the fits by PFO, PSO and Ver equations for the Pb^{2+} and Cd^{2+} adsorption onto AS and HS at the two particle sizes.

From a mere statistical point of view, the datasets at the two particle sizes for each investigated substrate/cation system resulted always different at a significance level of $\alpha = 0.05$ (*i.e.*, at a 95% confidence interval) for all the three fitting models. Despite this, from a practical and chemical perspective, the differences between the sorption capacity and the kinetics of the HS and AS particles at the two size intervals towards Cd^{2+} and Pb^{2+} ions are not so great (the slightly higher q_e and k values at the smaller particle size are attributable to their higher superficial area). Moreover, independently of the size, the adsorption equilibrium for both metal ions in the experimental conditions used was reached within 100 minutes. Therefore, the possibility of using the two raw materials with a higher particle size interval can be very useful from an applicative point of view, when, *e.g.*, HS or AS could be used as a stationary phase of a column, without altering dramatically their adsorption ability towards the toxic metal ions.

Apart that, considering the significant differences among all eight datasets (*i.e.*, 2 metal cations, for 2 substrates, for 2 particle sizes), the three kinetic models have been statistically compared separately

for each dataset. This kind of comparisons, even at a "minimum" level, should be encouraged, since, as commented elsewhere (Cataldo et al. 2016a), "the selection of a fitting model instead of another is often done without scientific criteria, but only for subjective reasons". By performing the *F*-test to compare the three models used on all the datasets of the kinetic experiments, some interesting aspects emerge (results shown in Table 3S).

The PFO is always significantly different than PSO and Ver models, except for the adsorption of Cd(II) on the small particle sizes of both AS and HS, for which PFO shows significant differences only with Ver model for the HS-Cd^{2+}-small dataset. Interestingly, PFO is always the model with the highest variance (*i.e.*, the worse for *F*-test), except in the case of the adsorption of Cd^{2+} on the two substrates at a big particle size, where the variance of PFO model is significantly lower than both PSO and Ver models, as an indication that the Pseudo First Order equation fits those datasets significantly better than the other two. Finally, the PSO and Ver models result to never be significantly different at that significance level, letting one conclude that both models can be indifferently used to describe the sorption kinetics of the investigated systems. Because of that, the Akaike Information Criteria were used to try to take a decision on the best model. Based on the AIC values reported in Table 2, we calculated the *Akw* for each fitting function for all the datasets, and also the probability that the selected model was better than another, based on eq. (14). It resulted, for each dataset, as follows:

1) "AS-Pb^{2+}-small": **PSO** is ~$1.06 \cdot 10^5$ and ~1.5 times more probable as best model than PFO and Ver, respectively (with Ver ~$7.27 \cdot 10^5$ times better than PFO);

2) "AS-Pb^{2+}-big": **Ver** is ~$1.25 \cdot 10^6$ and ~575 times more probable as best model than PFO and PSO, respectively (with PSO ~$2.18 \cdot 10^3$ times better than PFO);

3) "AS-Cd^{2+}-small": **PSO** is ~$1.85 \cdot 10^3$ and ~46 times more probable as best model than PFO and Ver, respectively (with Ver ~40 times better than PFO);

4) "AS-Cd^{2+}-big": **PFO** is ~$5.07 \cdot 10^{23}$ and ~$7.96 \cdot 10^{21}$ times more probable as best model than PSO and Ver, respectively (with Ver ~64 times better than PSO);

5) "HS-Pb^{2+}-small": **Ver** is ~$9.64 \cdot 10^8$ and ~$2.28 \cdot 10^3$ times more probable as best model than PFO and PSO, respectively (with PSO ~$4.22 \cdot 10^6$ times better than PFO);

6) "HS-Pb^{2+}-big": **Ver** is ~$5.61 \cdot 10^7$ and ~495 times more probable as best model than PFO and PSO, respectively (with PSO ~$1.13 \cdot 10^5$ times better than PFO);

7) "HS-Cd^{2+}-small": **Ver** is ~$5.55 \cdot 10^6$ and ~$2.11 \cdot 10^3$ times more probable as best model than PFO and PSO, respectively (with PSO ~263 times better than PFO);

8) "HS-Cd^{2+}-big": **PFO** is ~$1.98 \cdot 10^{10}$ and ~$1.05 \cdot 10^{11}$ times more probable as best model than PSO and Ver, respectively (with PSO ~5.3 times better than Ver).

Therefore, though PSO is usually preferred for the kinetic study of metal ions adsorption by different materials (Bulut and Tez 2007; Park et al. 2010; Taşar et al. 2014), Ver resulted the most probable model in most of the cases. In the few where PSO was favoured (*i.e.*, for the adsorption of both Pb^{2+} and Cd^{2+} on almond shells with small particle size), the probability that the former was better than the latter was always very low (only ~1.5 and ~46 times, for Pb^{2+} and Cd^{2+}, respectively). Interestingly, as already noted by the analysis of various *F*-tests, in the two cases where PFO was the preferred model (*i.e.*, for Cd^{2+} adsorption on the two substrates with big particle size), the probabilities were huge, meaning that PFO is substantially much better than the other two models. On the basis of the above considerations, comments on the results of the adsorption kinetics will be mainly based on the Ver model.

HS has a higher adsorption capacity towards Pb^{2+} ions, while the AS material preferentially adsorbs Cd^{2+} in the experimental conditions investigated (e.g., q_e = 5.3 10^{-3} and 5.6 10^{-3} mmol g^{-1} for Cd(II) and Pb(II) adsorption, respectively, by HS-small; $q_e = 8.2 \cdot 10^{-3}$ and $3.5 \cdot 10^{-3}$ mmol g^{-1} for Cd(II) and Pb(II) adsorption, respectively, by AS-small). These results are in agreement with those obtained from the semi-quantitative EDX analysis.

The adsorption rate of Cd^{2+} and Pb^{2+} on AS material is higher than that on HS (e.g., k_v = 0.01 and 0.02 min^{-1} for Cd(II) adsorption by HS-small and AS-small, respectively; k_v = 0.02 and 0.03 min^{-1} for Pb(II) adsorption by HS-small and AS-small, respectively).

3.4 Temperature effect on the Cd(II) and Pb(II) adsorption by AS and HS

The dependence on temperature of the adsorption isotherm of a sorbent material towards organic or inorganic substances is of fundamental importance in the comprehension of adsorption mechanism. Bulut and Tez have already studied this dependence in the temperature range 25 – 60 °C for the same metal – adsorbent systems here investigated (Bulut and Tez 2007). A very small increase of sorption ability with the increasing of temperature was found in each system (e.g., q_m = 5.42 and 5.47 mg g^{-1} for the Cd(II) – HS system at 25 and 60 °C, respectively). Unfortunately, the authors did not give information about the AS and HS cultivars. For this reason, with the aim to confirm their results, we carried out isotherm experiments in the same temperature range (25 – 60 °C), at pH = 5, in $NaNO_3$ medium and at I = 0.1 mol L^{-1}.

Langmuir, Freundlich and Sips isotherm equations were used to fit the experimental data. The fitting curves and the values of the refined parameters of the three isotherms are reported as supplementary material (Fig. 6S and Tables 4S and 5S). Sips equation was considered as the best model in terms of experimental data fit. Further details about this choice will be given in next sections.

According to the results of Bulut and Tez, in the temperature range 25 – 60 °C a slightly variation of q_m was observed in each system (*e.g.*, q_m = 1.6 and 2.3 mg g^{-1} for Cd^{2+} adsorption onto HS material, at T = 25 and 60 °C, respectively). The same consideration can be done for *Ks* values (*e.g.*, K_S = 0.05 and 0.03 L^s g^{-s} for the Pb^{2+} adsorption onto AS material, at T = 25 and 60 °C, respectively). Moreover, for both the parameters, the differences in data values calculated at the three temperatures are, almost always, of the same magnitude of experimental errors (see Table 3) and, as consequence, not significant.

Considering the low effect of this variable on the Pb^{2+} and Cd^{2+} adsorption by AS and HS, we focused our attention on other less-studied variables, like the ionic medium and ionic strength of the metal ion solution (see next section).

3.5. Data analysis of the adsorption isotherms at T = 25 °C

In order to evaluate the dependence on I of the sorption capacity of AS and HS towards the investigated metal ions, the adsorption equilibrium experiments at T = 25°C were carried out at pH=5, in NaCl at different ionic strengths ($0.05 \leq I$ / mol $L^{-1} \leq 0.5$). For comparison, some measurements were also carried out in $NaNO_3$ at I = 0.1 mol L^{-1}. Considering the slightly lower sorption capacity of the big particle size materials, and taking into account the "non dramatic" differences between the two sizes, only the small particle sizes were considered in the study. Langmuir, Freundlich and Sips isotherm equations were used to fit the experimental data, and the values of the refined parameters are reported in Tables 4 and 5 together with their errors, the correlation coefficients of single fits, as well as the standard deviation and the Akaike's values obtained from the simultaneous fit of all datasets of a given system at different ionic strengths. This approach, already used in previous studies (Cataldo et al. 2016a), has been followed to make statistical comparisons as much general as possible, in order to reach common conclusions about various fitting models on the different datasets, independently on the ionic strength. The plots of the experimental data together with the fitting curves are reported in Fig. 6 and in Figs 7S – 9S.

Results obtained for the fits of all the experimental data by the three models need to be carefully analyzed. In analogy to what has been done for the kinetic results, the *F*-test has also been performed to compare the three models used on all the datasets of the equilibrium experiments (results shown in Table 6S).

Looking at the Table, it emerges that Freundlich model is always significantly different (worse) than Sips, except for the adsorption of both Pb^{2+} and Cd^{2+} onto Hazelnut shells in $NaNO_3$ (differences not statistically significant at α = 0.05). Concerning Langmuir model, fitting resulted always better than Freundlich (see standard deviations in Tables 4-5), and generally worse than Sips, though the

differences between Langmuir and the other two models were not significant (except for the adsorption of Pb^{2+} onto both substrates in NaCl for the comparison of Freu/Lang, and for the adsorption of Cd^{2+} onto Almond shells in both media and onto Hazelnut shells in NaCl for the comparison of Lang/Sips). Moreover, another consideration is worth of mentioning when analyzing the fits by Langmuir and Sips equations. Looking at them (eqs. 8 and 9, respectively), it is evident how Sips only differs from Langmuir for the fact that the term C_e is powered to the reciprocal of the adjustable parameter *S*. Some of the fits reported in Tables 4 and 5 gave, as a result, refined *S* values close to "1", making Sips equation "coincident" with Langmuir. This fact is also proven by the model comparison by the Akaike's Information Criterion, which often gave relatively low probabilities (respect to other comparisons) that one among Sips and Lang was better than the other. In particular, AIC analysis gave the following results for each dataset:

1) "AS-Pb^{2+}-$NaNO_3$": **Sips** is ~$1.93\cdot10^3$ and ~4.2 times more probable as best model than Freu and Lang, respectively (with Lang ~462 times better than Freu);

2) "AS-Pb^{2+}-NaCl": **Lang** is ~$5.69\cdot10^6$ and ~320 times more probable as best model than Freu and Sips, respectively (with Sips ~$1.78\cdot10^4$ times better than Freu);

3) "AS-Cd^{2+}-$NaNO_3$": **Sips** is ~$1.49\cdot10^5$ and ~$7.61\cdot10^3$ times more probable as best model than Freu and Lang, respectively (with Lang ~19 times better than Freu);

4) "AS-Cd^{2+}-NaCl": **Sips** is ~$2.73\cdot10^{19}$ and ~$6.34\cdot10^{15}$ times more probable as best model than Freu and Lang, respectively (with Lang ~$4.31\cdot10^3$ times better than Freu);

5) "HS-Pb^{2+}-$NaNO_3$": **Lang** is ~375 and ~5.5 times more probable as best model than Freu and Sips, respectively (with Sips ~68 times better than Freu);

6) "HS-Pb^{2+}-NaCl": **Lang** is ~$6.88\cdot10^6$ and ~3.9 times more probable as best model than Freu and Sips, respectively (with Sips ~$1.76\cdot10^6$ times better than Freu);

7) "HS-Cd^{2+}-$NaNO_3$": **Sips** is ~46 and ~17 times more probable as best model than Freu and Lang, respectively (with Lang ~2.5 times better than Freu);

8) "HS-Cd^{2+}-NaCl": **Sips** is ~$7.05\cdot10^{10}$ and ~$5.49\cdot10^6$ times more probable as best model than Freu and Lang, respectively (with Lang ~$1.28\cdot10^4$ times better than Freu);

As a consequence of that, we can conclude that both Langmuir and Sips models can be equally used to comment results obtained. Only after this conclusion, since the latter is more "general" (as already stated, Sips "includes" Langmuir) than the former, it has been preferred to comment results.

In the ionic media and in the investigated ionic strength range, HS has a higher adsorption ability towards Pb^{2+} than Cd^{2+} (*e.g.* q_m=0.007 and 0.012 mmol g^{-1} in NaCl, at I = 0.25 mol L^{-1} for the adsorption onto HS of Cd(II) and Pb(II), respectively). Considering the experimental errors on the q_m values (see Tables 4 and 5), an opposite behaviour in the adsorption ability of AS toward the two

metal ions was found (*e.g.* q_m=0.015 and 0.010 mmol g^{-1} in NaCl, at I=0.25 mol L^{-1} for the adsorption onto AS of Cd(II) and Pb(II), respectively). In the two ionic media and at all ionic strengths, Cd(II) is better adsorbed by AS (*e.g.* q_m=0.007 and 0.015 mmol g^{-1} in NaCl, at I=0.25 mol L^{-1} for the Cd^{2+} adsorption onto HS and AS materials, respectively). The adsorption trends of AS and HS towards Pb(II) and Cd(II) are in general the same of those found at the other temperatures (see section 3.4). Differences in the adsorption capacity of HS and AS towards Pb^{2+} were found only in $NaNO_3$ medium and in NaCl at the lowest ionic strength values. In particular, in these experimental conditions, the HS shows a higher adsorption capacity towards Pb^{2+} ions than AS (*e.g.,* q_m=0.030 and 0.020 mmol g^{-1} in $NaNO_3$, at I=0.1 mol L^{-1} for the Pb^{2+} adsorption onto HS and AS materials, respectively). As in the kinetic experiments, the pH of metal ions solutions after contact with AS or HS varied of 0.2-0.3 units. The isotherms results, as well as the kinetic data, are in good agreement with the semi-quantitative results obtained from the analysis of EDX spectra. The analysis of the trend of q_m and K_i values (see Tables 4 and 5) clearly shows that the affinity of HS and AS towards the two metal ions plays the main role in the adsorption process, but this is not the only aspect that has to be considered. In fact, also the ionic medium composition and the ionic strength of the aqueous solution are responsible for a change in q_m and K_i values. In our investigations, the influence of chloride medium was evaluated. As reported in section 3.2, Pb(II) and Cd(II) ions form in NaCl medium differently charged chloride species, while, according to the literature data, no significant interactions occur with nitrate anion. Moreover, at the pH value used in our investigation (pH=5) no hydroxo species are formed by the two metal ions. The increase of chloride concentration reduces the percentage of the positively charged metal species (see Table 2S), which are able to interact with the binding groups of the sorbent materials. As a consequence, in NaCl medium, the amount of metal ion (Pb^{2+} or Cd^{2+}) adsorbed by AS and HS (q_m values) and the affinity of the adsorbent materials towards the metal ions (K_i) decreases with the increasing of ionic strength. The correlation between q_m and the percentage of positively charged species of metal ions in solution indicates an adsorption mechanism based on complexation reactions between the binding groups of the adsorbents (mainly –OH groups) and the toxic metal ions. The dependence of q_m parameter on chloride concentration has been modeled eq. 15

$$q_m = q_{m0} + \mathrm{p}\ C_{Cl^-}^{0.5} \qquad (15)$$

where q_{m0} is the q_m value at C_{Cl^-} = 0 and p is an empirical parameter. The q_{m0} and p values calculated for each investigated system are reported in Table 6 together with their errors and the std. dev. of the fits. By taking into account the errors on the parameters, the q_{m0} values calculated by eq. 15 are very close to the q_m obtained in $NaNO_3$ medium at I=0.1 mol L^{-1}. This confirms the goodness of q_m values obtained in $NaNO_3$ medium and, once again, the importance of considering the ionic medium of the solution containing the toxic metal ion when planning its removal by means of a bio-adsorption

process. As an example, Fig. 7 shows the trend of q_m values with the chloride concentration (C_{Cl^-}) together with the curve fits of the experimental data according to eq. 15, for the Cd^{2+}-AS and Cd^{2+}-HS systems. HS has a greater affinity for Pb^{2+} than AS, as confirmed by the highest K_i values calculated with the three isotherm models in the whole range of ionic strengths investigated. No important differences were found in the affinity (K_s values) of the two adsorbent materials towards Cd^{2+} ion.

3.6. Comparisons with literature data

Only a rough comparison can be done between the adsorption capacity (q_m) here obtained and those reported in literature. In fact, although the mean chemical composition of HS and AS used in this work is similar to that of other cultivars, small differences (*e.g.*, the different degree of fruit ripeness) can cause a change in their sorption capacity towards Pb^{2+} and Cd^{2+} ions. Moreover, also the pretreatments of the adsorbent materials, as well as the experimental conditions chosen in the adsorption experiments, play an important role (initial metal ion concentration, pH, ionic strength, ionic medium). The highest q_m variability was found for the Pb-HS system, with values that ranged between 7 mg g^{-1} found in this work and 41.9 mg g^{-1} by ~~Şencan et al.~~ (Şencan et al. 2015). In the most of the articles found in literature on this topic, sorption experiments were carried out in aqueous solutions at pH different than 5 and without ionic medium (see data reported in Table 7S). Considering the experimental differences above reported, a good accordance was found with q_m values reported by ~~Bulut et al. and Tez and Mehrasbi et al.~~ (Bulut and Tez 2007; Mehrasbi et al. 2009) for the same Cd^{2+}-AS and Pb^{2+}-AS systems. To the best of our knowledge, only ~~Pehlivan et al.~~ (Pehlivan et al. 2009) considered the effect of ionic strength on Pb(II) adsorption onto hazelnut and almond shells by using KNO_3 as ionic medium. Unfortunately, the authors did not report quantitative data at different ionic strengths. They only observed that the Pb^{2+} sorption decreases with the increasing of ionic strength and no important changes were noted in the ionic strength range 0.01-0.1 mol L^{-1}.

4. Conclusions

AS and HS have all the features of the ideal adsorbent material to be used in bioadsorption processes. In fact, they are environmental friendly, cheap, and highly available in Sicily. In this paper the two raw materials have been used to remove Pb(II) and Cd(II) ions from aqueous solutions in different experimental conditions. The results obtained can be summarized as follows:

1. AS and HS have been analyzed by TGA-DSC, SEM-EDX and FT-IR measurements in order to know the binding sites responsible of their sorption capacity towards metal ions, their

morphology and their (semi quantitative) composition before and after Pb(II) and Cd(II) adsorption;

2. a speciation study of the two metal ions in aqueous solution was made in the same experimental conditions (ionic medium, ionic strengths and pH) of adsorption experiments. The results, in terms of type, charge and percentage of each metal species have been used to explain the metal adsorption data;
3. the variation of the adsorption capacity of metal ions as a function of chloride concentration let us affirm that the interactions between positively charged metal species and negative or neutral binding sites of sorbent materials (*i.e.* complexation) play a fundamental role in the sorption process.
4. the kinetic and thermodynamic data on the metal ion sorption by AS and HS at the different experimental conditions were analyzed by the equations usually employed in literature, and a statistical evaluation was done to choose the best model in terms of data fit and interpretation;
5. important considerations were done about the influence of the ionic medium and its concentration on the adsorption process. An empirical equation was used to describe the trend of q_m parameter with the chloride concentration in solution;
6. only a slightly effect of temperature on the adsorption capacity (q_m) and on the affinity of AS and HS towards the two metal ions (K_i) was found in the range 25 – 60 °C;
7. an adsorption mechanism based on the formation of complex species between the positively charged species of toxic metal ions and the binding groups (mainly -OH) of AS and HS has been hypothesized;
8. the adsorption capacity of ground AS and HS here used towards Pb(II) and Cd(II) was compared with literature findings by taking into account, where specified, the experimental conditions.

Acknowledgements

We thank the Italian Ministero dell'Istruzione, dell'Università e della Ricerca (MIUR, PRIN project n. 2015MP34H3_003 and 2015MP34H3_004) for financial support.

References

Akaike H (1974) A new look at the statistical model identification. IEEE Trans Autom Control 19:716–723.

Allouch M, Alami M, Boukhlifi F (2014) Kinetic and energy study of thermal degradation of biomass materials under oxidative atmosphere using TGA, DTA and DSC.

Baes CF, Mesmer RE (1976) The hydrolysis of cations. Wiley

Blázquez G, Ronda A, Martín-Lara MA, et al (2015) Comparative study of isotherm parameters of lead biosorption by two wastes of olive-oil production. Water Sci Technol J Int Assoc Water Pollut Res 72:711–720.

Bulut Y, Tez Z (2007) Adsorption studies on ground shells of hazelnut and almond. J Hazard Mater 149:35–41.

Cataldo S, Cavallaro G, Gianguzza A, et al (2013a) Kinetic and equilibrium study for cadmium and copper removal from aqueous solutions by sorption onto mixed alginate/pectin gel beads. J Environ Chem Eng 1:1252–1260.

Cataldo S, Gianguzza A, Milea D, et al (2016a) Pb(II) adsorption by a novel activated carbon – alginate composite material. A kinetic and equilibrium study. Int J Biol Macromol 92:769–778.

Cataldo S, Gianguzza A, Pettignano A, et al (2012) Complex formation of copper(II) and cadmium(II) with pectin and polygalacturonic acid in aqueous solution. An ISE-H^+ and ISE-Me^{2+} electrochemical study. Int J Electrochem Sci 7:6722–6737.

Cataldo S, Gianguzza A, Pettignano A (2016b) Sorption of Pd(II) ion by calcium alginate gel beads at different chloride concentrations and pH. A kinetic and equilibrium study. Arab J Chem 9:656–667.

Cataldo S, Gianguzza A, Pettignano A, Villaescusa I (2013b) Mercury(II) removal from aqueous solution by sorption onto alginate, pectate and polygalacturonate calcium gel beads. A kinetic and speciation based equilibrium study. React Funct Polym 73:207–217.

Cataldo S, Muratore N, Orecchio S, Pettignano A (2015) Enhancement of adsorption ability of calcium alginate gel beads towards Pd(II) ion. A kinetic and equilibrium study on hybrid Laponite and Montmorillonite-alginate gel beads. Appl Clay Sci 118:162–170.

Cimino G, Passerini A, Toscano G (2000) Removal of toxic cations and Cr(VI) from aqueous solution by hazelnut shell. Water Res 34:2955–2962.

Crea F, Foti C, Milea D, Sammartano S (2013) Speciation of cadmium in the environment. Met Ions Life Sci 11:63–83.

Crompton TR (2006) Toxicants in Aqueous Ecosystems: A Guide for the Analytical and Environmental Chemist. Springer Science & Business Media

De Stefano C, Lando G, Milea D, et al (2010) Formation and Stability of Cadmium(II)/Phytate Complexes by Different Electrochemical Techniques. Critical Analysis of Results. J Solut Chem 39:179–195.

De Stefano C, Sammartano S, Mineo P, Rigano C (1997) Computer tools for the speciation of natural fluids. In: Marine Chemistry – An Environmental Analytical Chemistry Approach, Kluwer Academic Publishers. A. Gianguzza, E. Pelizzetti, S. Sammartano, Amsterdam, pp 71–83

Demirbas A (2008) Heavy metal adsorption onto agro-based waste materials: A review. J Hazard Mater 157:220–229.

Demirbaş A (2002) Fuel Characteristics of Olive Husk and Walnut, Hazelnut, Sunflower, and Almond Shells. Energy Sources 24:215–221.

Fu F, Wang Q (2011) Removal of heavy metal ions from wastewaters: A review. J Environ Manage 92:407–418.

Haykiri-Acma H, Yaman S (2012) Comparison of the combustion behaviours of agricultural wastes under dry air and oxygen. WIT Trans Ecol Environ 163:145–151. doi: 10.2495/WM120141

Ho YS, Ofomaja AE (2006) Pseudo-second-order model for lead ion sorption from aqueous solutions onto palm kernel fiber. J Hazard Mater 129:137–142.

INC International (2015) 2014/15 Global Statistical Review.

Kim N, Park M, Park D (2015) A new efficient forest biowaste as biosorbent for removal of cationic heavy metals. Bioresour Technol 175:629–632.

Kocabaş-Atakli ZÖ, Okyay-Öner F, Yürüm Y (2015) Combustion characteristics of Turkish hazelnut shell biomass, lignite coal, and their respective blends via thermogravimetric analysis. J Therm Anal Calorim 119:1723–1729.

Martin AR, Martins MA, da Silva ORRF, Mattoso LHC (2010) Studies on the thermal properties of sisal fiber and its constituents. Thermochim Acta 506:14–19. doi: 10.1016/j.tca.2010.04.008

Mehrasbi MR, Farahmandkia Z, Taghibeigloo B, Taromi A (2009) Adsorption of Lead and Cadmium from Aqueous Solution by Using Almond Shells. Water Air Soil Pollut 199:343–351.

Micke W (1996) Almond Production Manual. Regents of the University of California, Oakland, California: University of California

Militky J, Meloun M (2011) Statistical Data Analysis: A Practical Guide., AbeBooks. Woodhead Publishing Ltd, New Delhi - India

Monji AB, Ghoulipour V, Mallah MH (2016) Biosorption of Toxic Transition Metals and Radionuclides from Aqueous Solutions by Agro-Industrial Byproducts. J Hazard Toxic Radioact Waste 20:1–9.

Nguyen TAH, Ngo HH, Guo WS, et al (2013) Applicability of agricultural waste and by-products for adsorptive removal of heavy metals from wastewater. Bioresour Technol 148:574–585.

Nurchi VM, Villaescusa I (2008) Agricultural biomasses as sorbents of some trace metals. Coord Chem Rev 252:1178–1188.

OriginLab (2004) Origin (OriginLab, Northampton, MA).

Park D, Yun Y-S, Park JM (2010) The past, present, and future trends of biosorption. Biotechnol Bioprocess Eng 15:86–102.

Pehlivan E, Altun T, Cetin S, Iqbal Bhanger M (2009) Lead sorption by waste biomass of hazelnut and almond shell. J Hazard Mater 167:1203–1208.

Ramiah MV (1970) Thermogravimetric and differential thermal analysis of cellulose, hemicellulose, and lignin. J Appl Polym Sci 14:1323–1337.

Ronda A, Martín-Lara MA, Dionisio E, et al (2013) Effect of lead in biosorption of copper by almond shell. J Taiwan Inst Chem Eng 44:466–473.

Ruthven DM (1984) Principles of Adsorption and Adsorption Processes. John Wiley & Sons

Şen A, Pereira H, Olivella MA, Villaescusa I (2014) Heavy metals removal in aqueous environments using bark as a biosorbent. Int J Environ Sci Technol 12:391–404.

Şencan A, Karaboyacı M, Kılıç M (2015) Determination of lead(II) sorption capacity of hazelnut shell and activated carbon obtained from hazelnut shell activated with $ZnCl_2$. Environ Sci Pollut Res Int 22:3238–3248.

Skreiberg A, Skreiberg Ø, Sandquist J, Sørum L (2011) TGA and macro-TGA characterisation of biomass fuels and fuel mixtures. Fuel 90:2182–2197.

Taşar Ş, Kaya F, Özer A (2014) Biosorption of lead(II) ions from aqueous solution by peanut shells: Equilibrium, thermodynamic and kinetic studies. J Environ Chem Eng 2:1018–1026.

Volesky B (2003) Sorption and Biosorption. BV Sorbex, Inc., Montréal, St. Lambert, Québec, Canada

Wagenmakers E-J, Farrell S (2004) AIC model selection using Akaike weights. Psychon Bull Rev 11:192–196.

Zhang Y, Zhao J, Jiang Z, et al (2014) Biosorption of Fe(II) and Mn(II) ions from aqueous solution by rice husk ash. BioMed Res Int 2014:973095.

Table 1. Semi-quantitative elemental composition of the HS and AS before and after contact with the Pb(II) and Cd(II) solutions by EDX analysis.[a]

Sample	**Semi-quantitative elemental composition (w/w %)**			
	C	**O**	**Cd**	**Pb**
HS	71.44	28.56	-	-
HS/Cd(II)	68.81	27.75	3.44	-
HS/Pb(II)	67.63	26.86	-	5.51
	C	**O**	**Cd**	**Pb**
AS	70.78	29.22	-	-
AS/Cd(II)	67.25	26.23	6.52	-
AS/Pb(II)	67.34	26.84	-	5.82

[a] The percentages are the average of three EDX analysis with a mean error of 5%.

Table 2. Parameters of PFO, PSO and Ver kinetic equations for Pb^{2+} and Cd^{2+} adsorption on hazelnut and almond shell of two particle size intervals, in aqueous solution containing NaCl 0.1 mol L^{-1} and at T = 25°C.

		HS					AS				
Model	**Size**	q_e [a]	k_i [b,c]	R^2	σ [d]	*AIC* [e]	q_e [a]	k_i [b,c]	R^2	σ [d]	AIC [e]
						Cd(II)					
PFO	small	0.58±0.01	0.06±0.01	0.9768	0.02504	-149.563	0.87±0.01	0.09±0.01	0.9838	0.02800	-180.915
	big	0.55±0.01	0.05±0.01	0.9935	0.01219	-268.415	0.86±0.01	0.07±0.01	0.9926	0.01608	-491.245
PSO	small	0.63±0.01	0.14±0.01	0.9864	0.01920	-160.708	0.92±0.01	0.17±0.01	0.9909	0.02097	-195.958
	big	0.59±0.01	0.13±0.01	0.9700	0.02619	-221.002	0.91±0.01	0.13±0.01	0.9545	0.03993	-382.079
Ver	small	0.59±0.01	0.01±0.01	0.9934	0.01334	-176.016	0.89±0.01	0.02±0.01	0.9878	0.02430	-188.286
	big	0.55±0.01	0.01±0.01	0.9666	0.02764	-217.660	0.86±0.01	0.02±0.01	0.9603	0.03726	-390.386
						Pb(II)					
PFO	small	1.16±0.01	0.08±0.01	0.9821	0.03471	-196.787	0.70±0.02	0.11±0.02	0.9233	0.05359	-87.783
	big	1.12±0.01	0.07±0.01	0.9761	0.04984	-123.252	0.64±0.01	0.07±0.01	0.9521	0.04058	-96.679
PSO	small	1.22±0.01	0.11±0.01	0.9924	0.02254	-222.694	0.74±0.01	0.29±0.03	0.9819	0.02600	-110.923
	big	1.18±0.01	0.10±0.01	0.9921	0.02691	-146.528	0.68±0.01	0.19±0.02	0.9817	0.02510	-112.051
Ver	small	1.17±0.01	0.02±0.01	0.9955	0.01742	-238.159	0.72±0.01	0.03±0.01	0.9811	0.02662	-110.172
	big	1.13±0.01	0.02±0.01	0.9956	0.02003	-158.937	0.65±0.01	0.02±0.01	0.9917	0.01687	-124.759

[a] mg g^{-1}; [b] min^{-1} for both k_1 and k_v, g mg^{-1} min^{-1} for k_2; [c] subscript i is 1, 2 or v according to the model; [d] standard deviation of the fit; [e] Akaike's value of the fit.

Table 3. Parameters of Sips isotherm for the Pb^{2+} and Cd^{2+} adsorption onto HS and AS materials with small particle size from aqueous solution at pH = 5, in $NaNO_3$ at I = 0.1 mol L^{-1} and at T = 25, 40 and 60 °C.

		HS					AS				
Metal ion	T [a]	q_m [b]	K_S [c]	s	R^2	σ [d]	q_m [b]	K_S [c]	s	R^2	σ [d]
	25	1.6±0.3	0.01±0.01	0.66±0.07	0.9933	0.02489	2.7±0.1	0.01±0.01	0.59±0.04	0.9964	0.04265
Cd(II)	40	1.8±0.6	0.02±0.01	0.7±0.2	0.9941	0.03376	4±1	0.02±0.01	0.6±0.2	0.9858	0.12673
	60	2.3±0.7	0.07±0.02	1.0±0.4	0.9960	0.03391	4.0±0.2	0.01±0.01	0.52±0.04	0.9979	0.06066
	25	6.2±0.8	0.04±0.01	0.90±0.08	0.9947	0.08443	4.2±0.3	0.05±0.01	0.78±0.06	0.9961	0.06212
Pb(II)	40	6±1	0.11±0.01	1.11±0.08	0.9989	0.05040	4.7±0.3	0.04±0.01	0.74±0.06	0.9984	0.05263
	60	6.4±0.7	0.12±0.01	0.9±0.1	0.9958	0.11636	5.2±0.6	0.03±0.01	0.71±0.09	0.9950	0.10564

[a] °C; [b] mg g^{-1}; [c] L^s mg^{-s}; [d] standard deviation of the whole fit.

Table 4. Parameters of Freundlich (Freu), Langmuir (Lang) and Sips isotherms for the Pb^{2+} adsorption on HS and AS materials with small particle size from aqueous solution at pH = 5 containing NaCl at different ionic strengths or $NaNO_3$ at I = 0.1 mol L^{-1} and at T = 25°C.

		HS						AS					
I [a]	**Model**	q_m [b]	K_i [c,d]	n (or s)	R^2	σ [e]	AIC [f]	q_m [b]	K_i [c,d]	n (or s)	R^2	σ [e]	AIC [f]
						$NaNO_3$							
	Sips	6.2± 0.8	0.04 ± 0.01	0.90 ± 0.08	0.9947	0.08443	-49.061	4.2±0.3	0.05 ± 0.01	0.78 ± 0.06	0.9961	0.06212	-49.968
0.10	Lang	7.3± 0.6	0.04 ± 0.01		0.9946	0.08459	-52.467	5.9±0.4	0.05 ± 0.01		0.9928	0.08463	-47.109
	Freu		0.39 ± 0.04	1.39 ± 0.07	0.9856	0.13862	-40.612		0.38 ± 0.04	1.48 ± 0.09	0.9781	0.14781	-34.840
						NaCl							
0.05		5.3±0.7	0.14±0.02	1.10±0.08	0.9967			3.7±0.7	0.06±0.01	1.0±0.1	0.9928		
0.10		3.7±0.9	0.14±0.02	1.2±0. 2	0.9909			2.5±0.2	0.04±0.01	0.7±0.1	0.9908		
0.25	Sips	2.4±0.7	0.07±0.01	1.1±0.2	0.9932	0.04619	-246.486	2.0±0.6	0.02±0.01	0.9±0.2	0.9993	0.05086	-206.119
0.50		0.84±0.07	0.01±0.01	0.54±0.07	0.9944			1.0±0.3	0.01±0.01	0.7±0.2	0.9994		
0.05		4.5±0.2	0.16±0.01		0.9963			3.6±0.1	0.06±0.01		0.9935		
0.10		2.8±0.1	0.16±0.02		0.9890			3.0±0.1	0.06±0.01		0.9898		
0.25	Lang	2.1±0.1	0.07±0.01		0.9937	0.04997	-249.209	2.35±0.08	0.02±0.01		0.9994	0.05049	-217.656
0.50		1.6±0.2	0.03±0.01		0.9871			1.52±0.07	0.01±0.01		0.9950		
0.05			0.70±0.04	1.64±0.08	0.9884				0.37±0.03	1.8±0.1	0.9864		
0.10			0.50±0.03	1.9±0.1	0.9842				0.40±0.05	2.2±0.2	0.9763		
0.25	Freu		0.21±0.01	1.66±0.08	0.9897	0.07147	-217.721		0.11±0.01	1.62±0.05	0.9990	0.07523	-186.148
0.50			0.08±0.01	1.4±0.1	0.9800				0.04±0.01	1.44±0.09	0.9957		

[a] mol·L^{-1}; [b] mg g^{-1}; [c] $L^{1/n}$ g^{-1} $mg^{1-1/n}$ for K_F, L·mg^{-1} for K_L and L^s mg^{-s} for K_S; [d] subscript i is F, L or S according to the model; [e] standard deviation of the whole fit; [f] Akaike's value of the whole fit.

Table 5. Parameters of Freundlich (Freu), Langmuir (Lang) and Sips isotherms for the Cd^{2+} adsorption on HS and AS materials with small particle size from aqueous solution at pH = 5 containing NaCl at different ionic strengths or $NaNO_3$ at I = 0.1 mol L^{-1} and at T = 25°C.

		HS						AS					
I [a]	**Model**	q_m [b]	K_i [c,d]	n (or s)	R^2	σ [e]	AIC [f]	q_m [b]	K_i [c,d]	n (or s)	R^2	σ [e]	AIC [f]
						$NaNO_3$							
	Sips	1.6± 0.3	0.01 ± 0.01	0.66±0.07	0.9933	0.02489	-94.353	2.7±0.1	0.01±0.01	0.59±0.04	0.9964	0.04265	-72.433
0.10	Lang	8± 4	0.01 ± 0.01		0.9876	0.03377	-88.622	7±1	0.02±0.01		0.9819	0.09553	-54.561
	Freu		0.04 ± 0.01	1.05±0.05	0.9858	0.03616	-86.713		0.16±0.02	1.22±0.08	0.9714	0.12011	-48.607
						NaCl							
0.05		1.1±0.1	0.01±0.01	0.61±0.09	0.9831			2.4±0.2	0.02±0.01	0.55±0.05	0.9923		
0.10	Sips	0.84±0.04	0.01±0.01	0.55±0.07	0.9957	0.02094	-419.720	2.0±0.1	0.01±0.01	0.48±0.05	0.9905	0.04730	-289.061
0.25		0.78±0.09	0.01±0.01	0.58±0.07	0.9886			1.63±0.06	0.01±0.01	0.42±0.03	0.9931		
0.50		0.43±0.06	0.01±0.01	0.63±0.08	0.9914			1.41±0.09	0.01±0.01	0.47±0.04	0.9936		
0.05		2.5±0.5	0.02±0.01		0.9746			13±9	0.01±0.01		0.9734		
0.10	Lang	1.9±0.2	0.02±0.01		0.9805	0.02944	-388.685	5±1	0.03±0.01		0.9560	0.10491	-216.289
0.25		2.1±0.6	0.02±0.01		0.9775			3.4±0.7	0.04±0.01		0.9512		
0.50		1.1±0.2	0.01±0.01		0.9861			5±2	0.01±0.01		0.9662		
0.05			0.07±0.01	1.3±0.1	0.9658				0.12±0.02	1.05±0.07	0.9697		
0.10	Freu		0.06±0.01	1.30±0.09	0.9698	0.03475	-369.763		0.17±0.04	1.3±0.1	0.9352	0.12361	-199.553
0.25			0.04±0.01	1.19±0.09	0.9705				0.17±0.04	1.4±0.1	0.9247		
0.50			0.02±0.01	1.21±0.07	0.9816				0.08±0.02	1.1±0.1	0.9571		

[a] mol·L^{-1}; [b] mg g^{-1}; [c] $L^{1/n}$ g^{-1} $mg^{1-1/n}$ for K_F, L·mg^{-1} for K_L and L^s mg^{-s} for K_S; [d] subscript i is F, L or S according to the model; [e] standard deviation of the whole fit; [f] Akaike's value of the whole fit.

Table 6. q_{m0} and p parameters of eq. 15

System	q_{m0}[a]	p	σ[b]
Cd^{2+}-HS	1.4±0.1	-1.3±0.3	0.0657
Pb^{2+}-HS	6.8±0.4	-8.5±0.7	0.2937
Cd^{2+}-AS	2.7±0.2	-1.9±0.4	0.0972
Pb^{2+}-AS	4.5±0.3	-5.0±0.6	0.2628

[a] mg g^{-1}; [b] standard deviation on the whole fit.

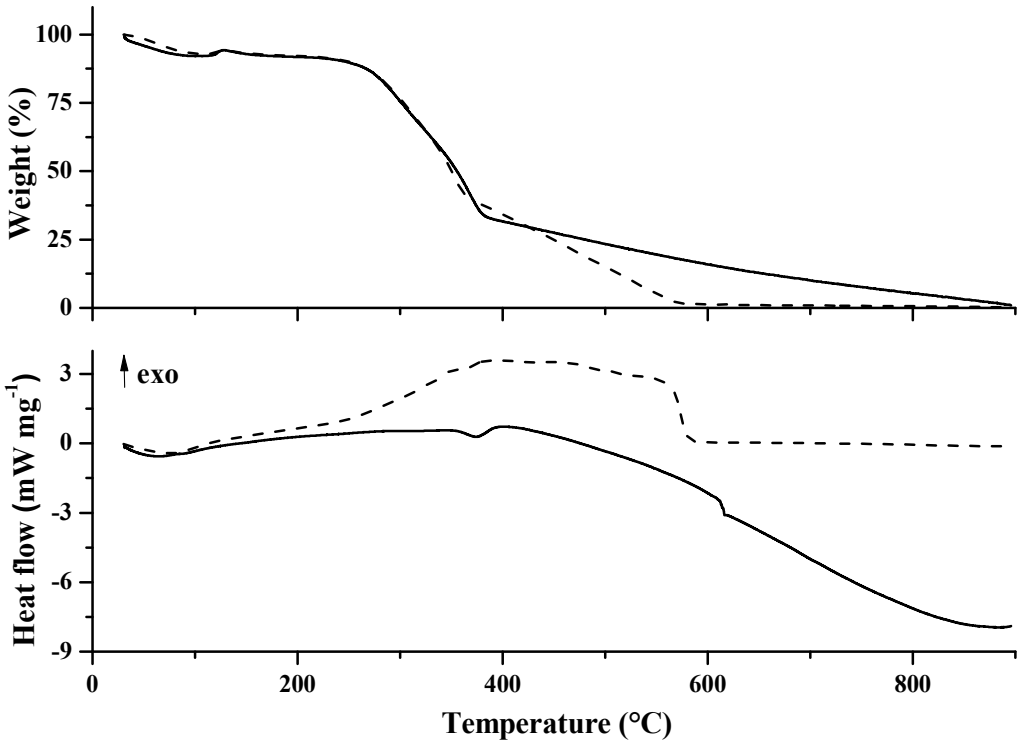

Figure 1. TGA-DSC curves of AS (straight lines) and HS (dashed lines) materials.

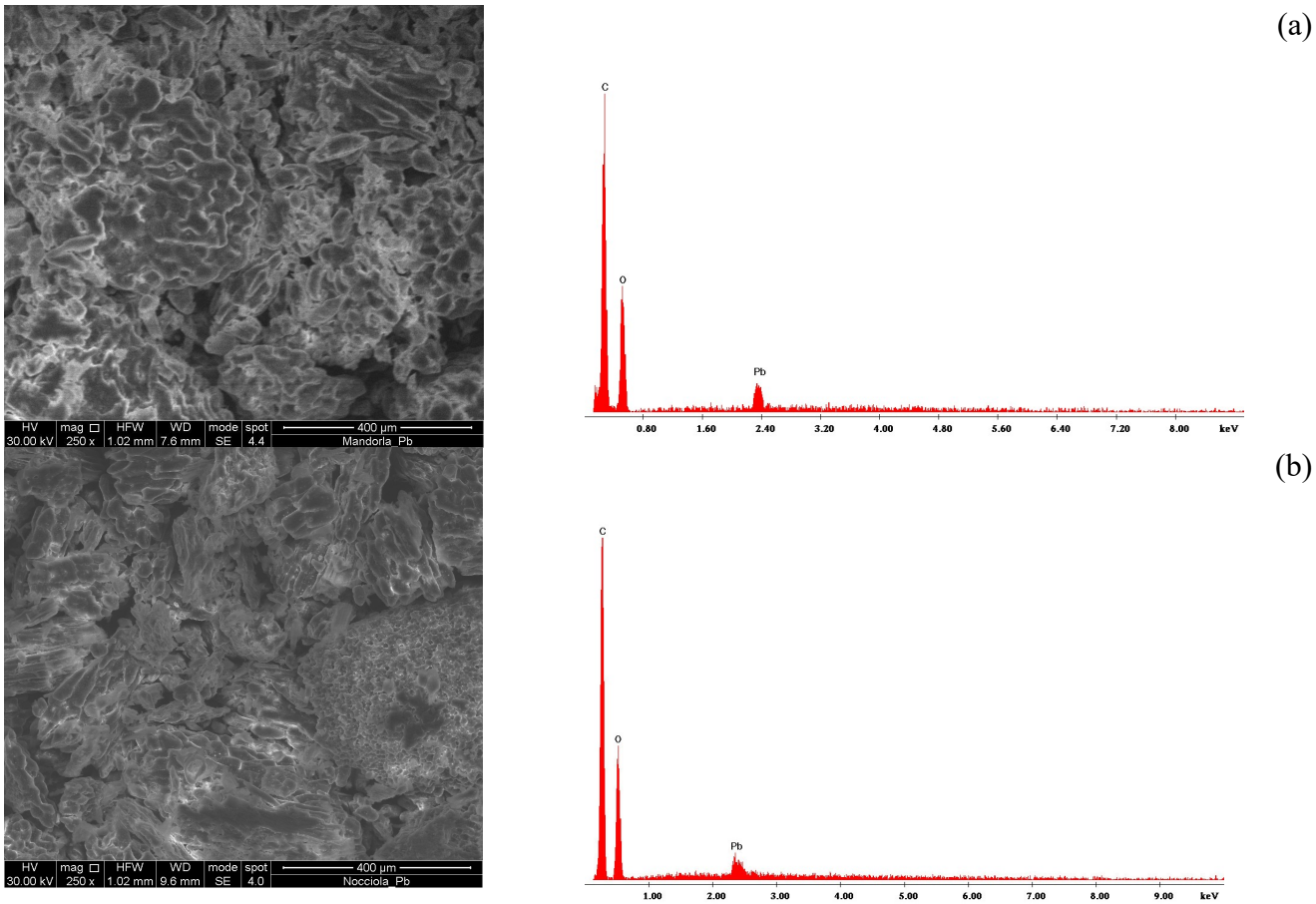

Figure 2. SEM micrographs obtained at 250x and EDX spectra of AS (a) and HS (b) after contact for 24 h with an aqueous solution at pH = 5 containing NaCl 0.1 mol L^{-1} and $Pb(NO_3)_2$ $C_{Pb^{2+}}$=30 mg L^{-1}.

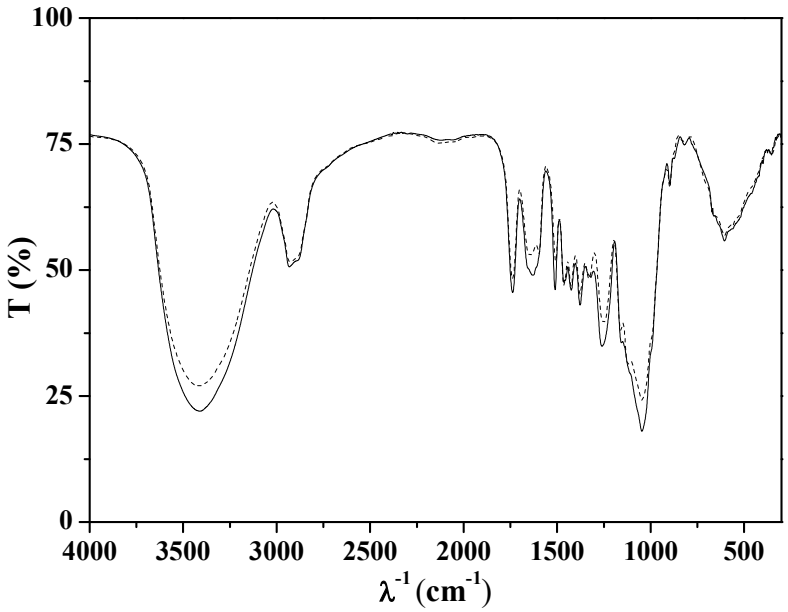

Figure 3. FT-IR spectra of HS (-) and AS (···) materials.

(a)

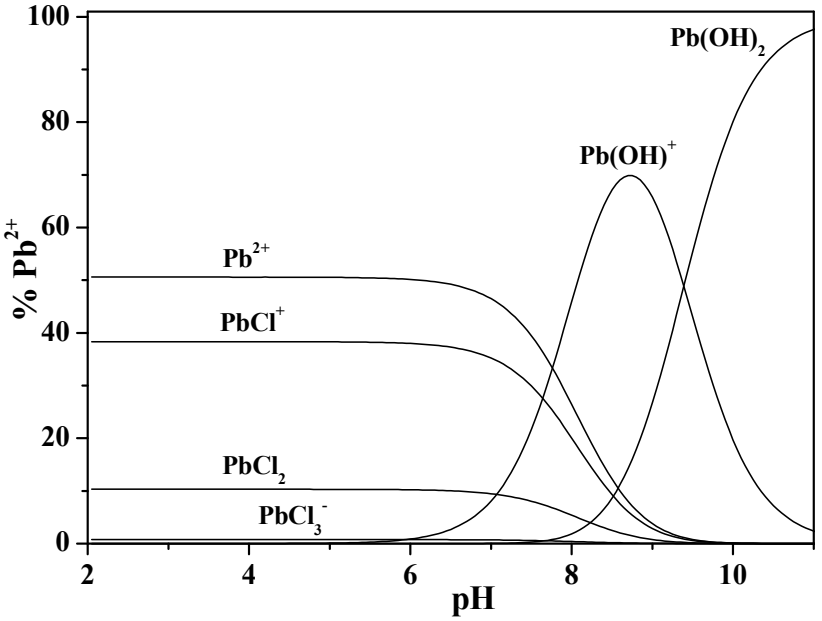

(b)

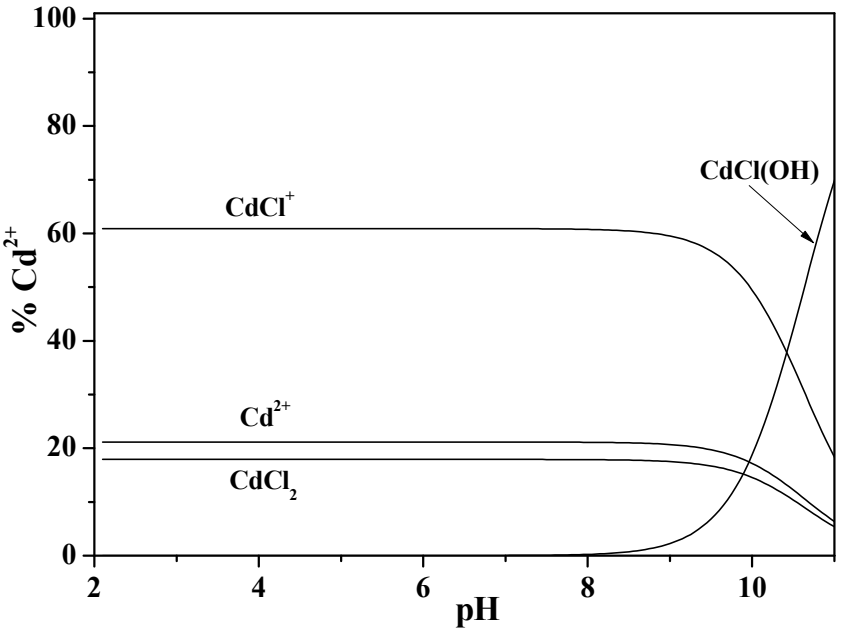

Figure 4. Distribution diagrams of Pb^{2+} (4a) and Cd^{2+} (4b) species *vs.* pH in $NaCl_{aq}$, at I = 0.1 mol L^{-1} and T = 25°C. Experimental details: $C_{Pb^{2+}}$ or $C_{Cd^{2+}}$=30 mg L^{-1}. The species reported in the two diagrams refer to the equilibrium: M^{2+} + p Cl^- + q H_2O = $MCl_p(OH)_q$ + q H^+, with M^{2+} = Pb^{2+} or Cd^{2+}, p and q are the stoichiometric coefficients and can assume integer values between 0 and n.

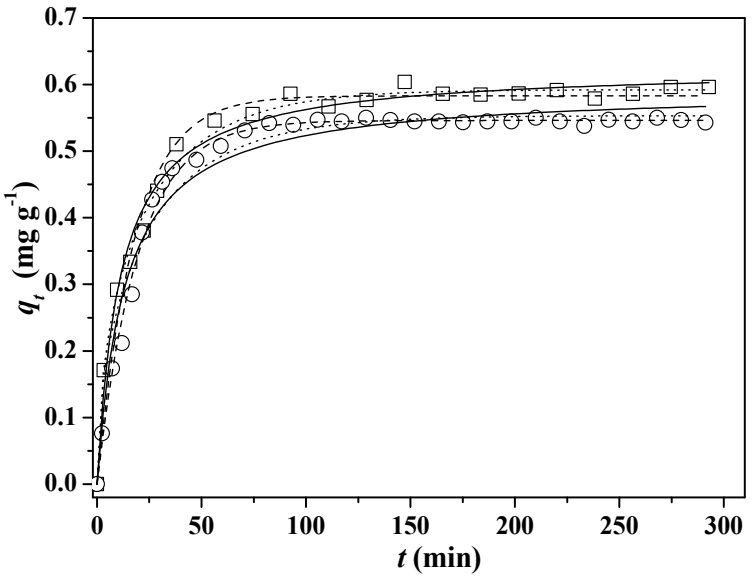

Figure 5. Dependence of q_t (mg g^{-1}) on contact time for Cd/HS system. Data are fitted with PFO (dashed line) PSO (continuous line) and Ver (dotted line) kinetic equations.

Experimental conditions: HS small (□) and big (○); ionic strength 0.1 mol L^{-1} (NaCl); $Cd(NO_3)_2$ ($C_{Cd^{2+}}$=30 mg L^{-1}); solution pH = 5; T = 25°C

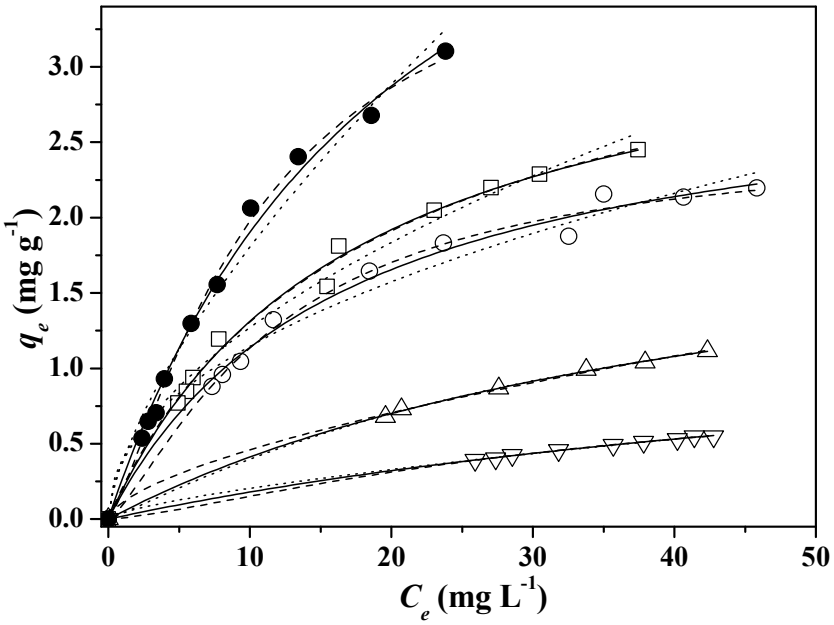

Figure 6. Adsorption isotherms of Pb^{2+} on AS with particle size interval $0.40 < x / \text{mm} \leq 1.18$ from aqueous solutions at pH = 5 containing NaCl 0.05 (□), 0.1 (○), 0.25 (Δ) and 0.5 (∇) mol L^{-1} and $NaNO_3$ 0.1 mol L^{-1} (●) and at T = 25°C. Experimental data fitted with Freundlich (dotted lines), Langmuir (continuous lines) and Sips (dashed lines) models.

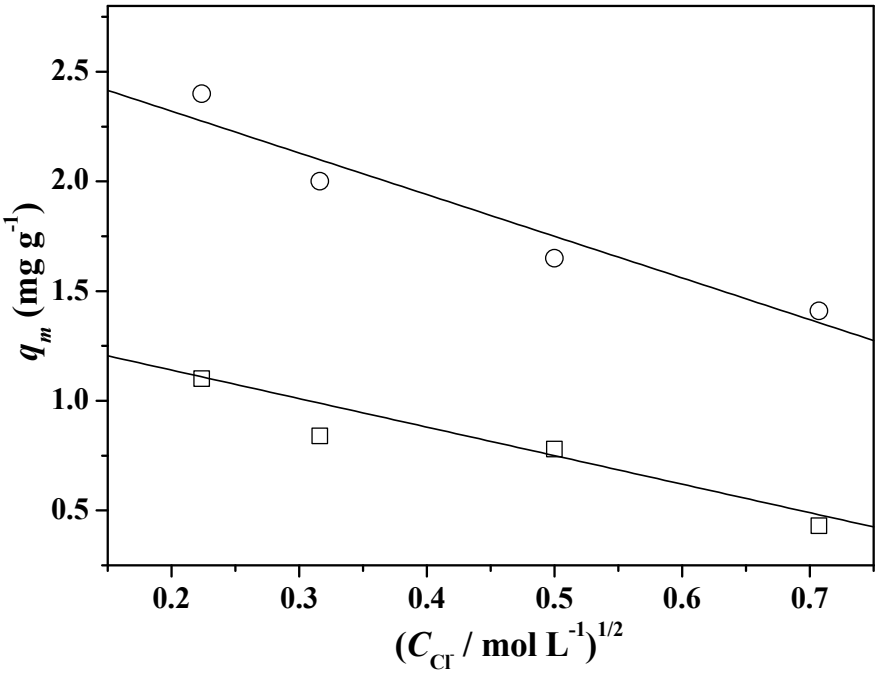

Figure 7. Dependence of q_m on $C_{Cl^-}^{0.5}$ for the adsorption of Cd(II) onto AS (○)and HS (□) materials at T = 25°C. The q_m value at C_{Cl^-} = 0 (q_{m0}) was calculated by using experimental q_m values and applying eq. 15.